2022 IEEE 18th International Conference on Automation
Science and Engineering (CASE)
August 20-24, 2022. Mexico City, Mexico

Stress-Aware Optimal Placement of Actuators for Ultra-High Precision Quality Control of Composite Structures Assembly

Areej AlBahar[1,3], Inyoung Kim[2], Tim Lutz[3], and Xiaowei Yue*[3]

***Abstract*— Modeling stress-induced processes is challenging and extremely critical in the quality control of advanced manufacturing systems. While residual stresses may be beneficial in some situations, in composite structures assembly, high residual stresses and extreme deformations are crucial and must be accounted for to prevent future catastrophic failures. Currently, conventional approaches to the optimal placement of actuators on composite structures are non-optimal, require ten actuators heuristically, and are insufficient in considering residual stresses. To overcome these limitations, we propose a *Stress-Aware Optimal Actuator Placement framework*. The stress-aware optimal actuator placement framework is able to achieve significant reductions of at least 39.3% in mean root mean squared deviations (RMSD) and 52% in maximum forces (MF), and only requires eight actuators on average while satisfying the safety threshold of residual stresses.**

***Index Terms*— Bayesian optimization, composite structures assembly, physical constraints, residual stress**

I. Introduction

The rapid growth in the development and use of composite materials has undoubtedly proved their success in various industrial areas, such as aerospace, automotive, and structural engineering. A composite material is a heterogeneous material composed of two or more components. Composite materials with different components have heterogeneous mechanical properties [1], [2]. Carbon Fiber-Reinforced Polymer (CFRP) is one of the most widely used composite materials in the aerospace industry. CFRPs have outstanding mechanical properties such as light weight, high fatigue, and tensile strengths. In the aerospace industry, for example, composite structures constitute more than 50% by weight of the Boeing 787 and Airbus 350 [3], as shown in Fig. 1 (a) [4]. Although composites have great properties that distinguish them from other materials, they are anisotropic and heterogeneous. Meanwhile, dimensional deviations inevitably exist due to manufacturing variability, different batches, or different suppliers, as shown in Fig. 1 (b-d) [5], [6]. These challenges make the quality control of composites assembly processes very challenging. An important factor to impact the quality of a composite structure is the placement of actuators.

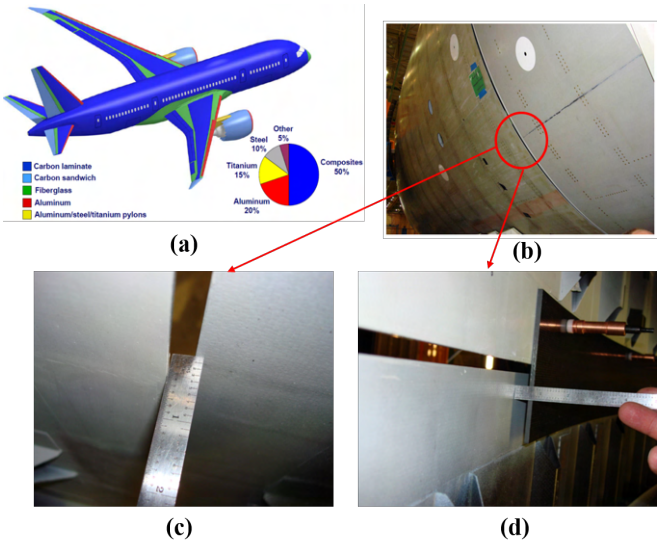

Fig. 1. **Aerospace composite structures: (a) composites account for 50% in Boeing 787, (b-d) dimensional gap existed during initial joining of two structures.**

In aerospace manufacturing, the placement of actuators is the process of placing actuator forces on the edge of the outer shell of a pre-assembled composite fuselage, as shown in Fig. 2. This process is carried out by pushing/pulling the composite structure, via robotic actuators, such that deviations to the intended design are as small as possible. A fuselage, a carbon fiber-reinforced composite, represents the main part of the airplane (i.e., the part holding crew, passengers, and cargo). The structural deviations along with the heterogeneity and anisotropicity of such composites make the placement of actuators on composite structures an extremely challenging process. The placement of actuators has a significant impact on the quality control of aircraft assembly. Moreover, the inappropriate placement of actuators may cause extreme distortions at some locations resulting in residual stresses. The mechanical properties of a composite structure are significantly affected by the formation of residual stresses.

Residual stresses are usually inevitable after joining two structures and releasing actuators. Large residual stresses affect the inner bond of composite structures, which may cause, debonding, micro-cracking, and degradation, or even lead to a catastrophic failure of the part prior to its intended lifetime. Hence, accounting for residual stresses when

*This work was supported by National Science Foundation under Grant No. 2035038, Grainger Frontiers of Engineering Grant Award from the National Academy of Engineering (NAE), and ICTAS Diversity and Inclusion Award and Virginia CCAM Innovation Fund. (Corresponding author: Dr. Xiaowei Yue.)

[1] Areej AlBahar is with the Department of Industrial and Systems Engineering, Virginia Tech, Blacksburg, VA, 24061, and the Department of Industrial and Management Systems Engineering, Kuwait University, Kuwait. areejaa3@vt.edu

[2] Inyoung Kim is with the Department of Statistics, Virginia Tech, Blacksburg, VA, 24061. inyoungk@vt.edu

[3] Tim Lutz and Xiaowei Yue are with the Department of Industrial and Systems Engineering, Virginia Tech, Blacksburg, VA, 24061. tlutz@vt.edu and xwy@vt.edu

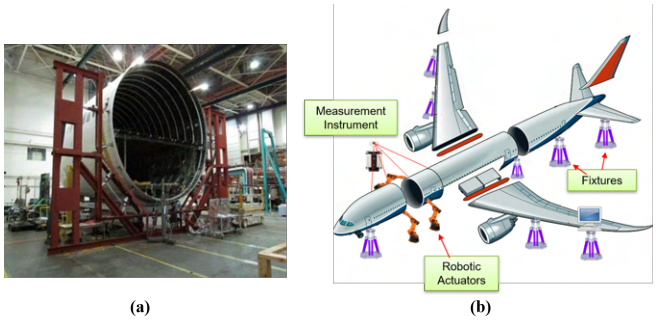

(a) (b)

Fig. 2. **(a) Actuators in the shape control of a fuselage [15], (b) robotic actuators scheme in the aircraft assembly.**

placing the actuators on composite structures is pivotal in aerospace manufacturing. To study and analyze the failure of composite materials and structures, many residual stress failure criteria have been developed. Tsai-Hill [7], Hashin-Rotem [8], and Tsai-Wu [9], are all mechanics-based failure criteria that have been used extensively over the past years. In this paper, we use the Tsai-Wu criterion for its nice mathematical representation, effectiveness, and generalization of other failure criteria (e.g., Tsai-Hill).

Researchers have spent years working on optimizing the placement of actuators in structural and control design [10], linear systems [11], vibration control [12], and actively controlled structures [13]. However, little research has been done on the placement of actuators on composite fuselages. A shape control system has been proposed to adjust the dimensional shape during the aircraft assembly, and a finite element model was developed to evaluate the feasibility and shape control performance [14]. Surrogate model based control has been proposed to reduce the deviations between two pre-assembled composite fuselages to an acceptable precision [15], [16]. In these existing work and current practices, the best fixed actuator placement policy, a scheme based on engineering domain knowledge and heuristics, is used to place ten actuators equally spaced from each other on a composite fuselage to reduce dimensional deviations [15]. Recently, a sparse learning based optimal actuators placement approach was developed [17]. This method uses the Alternating Direction Method of Multipliers (ADMM) to learn parameters and then use the sparse learning to efficiently identify the best locations for ten actuators to enable the composite fuselage shape control. Although these approaches have reduced the deviations of incoming fuselages, they require a fixed number of actuators (i.e., ten actuators), and do not include residual stresses in the optimization process. To overcome these limitations, we investigate the use of constrained Bayesian optimization with Gaussian processes (GPs) and propose a new framework to optimize the placement of actuators for the ultra-high precision (usually smaller than 0.01 inches) quality control of composite structures.

In this paper, we propose a *Stress-Aware Optimal Actuator Placement* approach by incorporating engineering-driven physical thresholds into constrained Bayesian optimization. Our approach provides flexibility to the number of actuators used in the placement scheme as well as constrains the optimization process by restricting residual stresses through a mechanics-driven safety threshold. We summarize our contributions as follows.

1. We propose a Stress-Aware Optimal Actuator Placement framework for ultra-high precision quality control of composite structures. This method incorporates the impact of residual stresses in the actuator placement problem.
2. We develop a computational algorithm to identify the global optimum for the actuator placement on composites structures problem.
3. The proposed method provides flexibility in the number of actuator forces applied, advances the quality control, and lays a solid foundation for system automation of robotic actuating.

The remainder of the paper is organized as follows: Section II discusses the proposed optimal actuator placement framework, Section III represents the case study of the placement of actuators on composite structures, Section **??** discusses the computational convergence property of our methodology, and Section IV validates the proposed algorithm. Finally, a brief summary is provided in Section V.

II. Stress-Aware Optimal Placement of Actuators

In this section, we present the generalized stress-aware optimal actuator placement for ultra-high precision quality control.

A. Problem Definition

The stress-aware optimal placement framework is formulated as follows: (1) we have a total of N measurement points (i.e., the points where deviations could be measured), and (2) we have m possible locations for actuator forces to be placed. We build our optimization framework upon the adjusted shape deviations response surface function introduced in [17]. The adjusted shape deviations' function shown in Equation 1 is based on the physical assumption that deformations and applied forces are linearly related in mechanics.

$$\delta = \Psi + UF, \tag{1}$$

where δ is an $(i \times 1)$ vector representing the adjusted shape deviations at N measurement points, Ψ is an $(i \times 1)$ vector representing the initial shape distortions, and U is an $(i \times j)$ displacement matrix. The vector $F = [\omega_1 F_1, \omega_2 F_2, .., \omega_j F_j]$ is a $(j \times 1)$ vector representing the designed forces, where ω_j is a binary variable representing the indicator whether an actuator force is placed at location j. In this paper, we aim to minimize the mean squared adjusted shape deviations δ^2.

In the proposed optimal placement strategy, the constraint functions are decided based on engineering safety thresholds, structural mechanics, and other domain knowledge. The

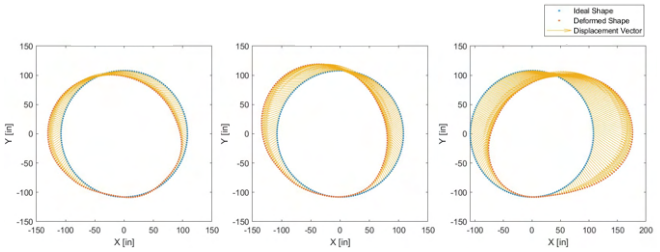

Fig. 3. **DOE simulations of real deformed composite fuselages.**

constraint functions of our proposed optimization framework are shown in Equations 2, 3, 4, and 5.

$$\sum_{j=1}^{m} \omega_j \leq M, \tag{2}$$

$$S \leq s, \tag{3}$$

$$F_{min} \leq F_j \leq F_{max}, \tag{4}$$

$$\omega_j = \begin{cases} 1 \text{ If an actuator is placed at position j} \\ 0 \text{ Otherwise.} \end{cases} \tag{5}$$

Too many actuators may result in an over-control issue. Therefore, Equation 2 constrains the total number of placed actuators to be less than or equal to a pre-specified threshold M. According to failure criteria of structural mechanics, Equation 3 restricts the maximum residual stress to a pre-specified safety threshold denoted as s. Equations 4, and 5 represent the upper and lower limits of each actuator force and the constraint on placements, respectively. The actuator force limits are influenced by two factors: one is the configurations of selected actuators, and the other is the safety threshold that was pre-specified by domain experts. Equations 4, and 5 are also considered as input search space for the constrained Bayesian optimization model.

B. Surrogate Modeling for Key Parameter Learning

We use surrogate models such as multivariate linear and Gaussian process regression models to find the displacement matrix U and residual stresses S. Firstly, we use the design of experiments (DOE) to simulate deformed composite structures. Three examples are shown in Fig. 3. The magnitude of deformation is comparable to the dimensional deviations in real composite structures. In Fig. 3, the ideal shape, shown in blue, and deformed shape, shown in red, are magnified 25 times for better visualization. Based on the physical assumption of the linear relationship between distortions and applied forces in mechanics, we find the displacement matrix U by solving the ordinary least-squares estimation of the linear regression model shown in Equation 6.

$$Y_i = F_D \beta_i + \epsilon_i, \tag{6}$$

where Y_i represents the design shape distortion vector at each measurement point i and F_D represents the design actuators force matrix at the m possible locations. The vector ϵ_i represents the residual term of the regression model and is assumed to follow a normal distribution. The displacement matrix U represents a vector of the estimated regressors β_i's (i.e., $[U = [\beta_1, \beta_2, .., \beta_N]$).

The residual stresses S are found by modeling the main pattern $f(Y)$ as a Gaussian process model in Equations 7 and 8.

$$S = f(Y) + e, \tag{7}$$

$$f(Y) \sim \mathcal{GP}(m(Y), k(Y, Y')), \tag{8}$$

where e represents the error term and is assumed to follow a normal distribution, and $m(Y)$ and $k(Y, Y')$ represent the mean function and kernel function of the Gaussian process model, respectively.
The mean $m(Y)$ and covariance $k(Y, Y')$ have the following expressions

$$m(Y) = E[f(Y)],$$
$$k(Y, Y') = E[(f(Y) - m(Y))(f(Y') - m(Y'))].$$

Furthermore, for any point Y_*, the joint Gaussian distribution of $f(Y)$ and $f(Y_*)$ is expressed as follows:

$$\begin{pmatrix} f(Y) \\ f(Y_*) \end{pmatrix} \sim \mathcal{N}\left(\begin{pmatrix} m(Y) \\ m(Y_*) \end{pmatrix}, \begin{pmatrix} k(Y,Y) & K(Y,Y_*) \\ k(Y_*,Y) & K(Y_*,Y_*) \end{pmatrix} \right),$$

where $K(.,.)$ denotes the *Gram matrix* of the kernel function $k(.,.)$. The closed form of the posterior distribution of $f(\cdot)$, using the properties of the normal distribution, can then be expressed as:

$$\tilde{f}(Y_*) \sim \mathcal{N}(\tilde{m}(Y_*), \tilde{\Sigma}(Y_*)),$$

where

$$\tilde{m}(Y_*) = m(Y_*) + k(Y_*, Y)k(Y, Y)^{-1}(f(Y) - m(Y)),$$
$$\tilde{\Sigma}(Y_*) = k(Y_*, Y_*) - k(Y_*, Y)k(Y, Y)^{-1}k(Y, Y_*),$$

where $\tilde{m}(Y_*)$ and $\tilde{\Sigma}(Y_*)$ are the posterior mean and covariance, respectively.

C. Constrained Bayesian Optimization (CBO)

In the proposed constrained Bayesian optimization for optimal actuators placement, the goal is to optimize the unknown and expensive-to-evaluate objective function, $f(x)$, subject to a set of constraints, $c_r(x)$'s, with respect to the input domain D_x as shown below.

$$min\ f(x)\ \forall\ x \in D_x,$$
$$s.t.\ c_r(x) \leq 0\ \forall\ r \in [1, .., R],$$

where $f(x)$ is associated with the main pattern of residual stresses and $c_r(x)$'s represents the physics-driven constraints associated with Equations 2 and 3. $f(x)$ and $c_r(x)$'s are expensive-to-evaluate functions modeled as GPs as shown in Equations 9 and 10, and R represents the total number of constraints.

$$f(x) \sim \mathcal{GP}(m(x), k(x, x')), \tag{9}$$

$$c_r(x) \sim \mathcal{GP}(\mu_r(x), \sigma_r(x))\ \forall\ r \in [1, .., R]. \tag{10}$$

We model the response surface variable y, for every input k, in Bayesian optimization as $y_k = f(\boldsymbol{x}_k) + \varepsilon_k$, where ε_k is

the error term at point k and is assumed to follow a GP model (i.e., $\varepsilon_k \sim GP(0, \Sigma^2)$). In CBO, to optimize the objective function, a constrained acquisition function is used to acquire the next point to be evaluated from the feasible input search space. We use the constrained expected improvement [18] as the constrained acquisition function, which we denote as cEI.

In CBO, each constraint function, given x, is modeled as a conditional independent Gaussian process model, thus, the posterior distribution of each constraint function, $c_r(x)$, is normal. Under this assumption, the constrained expected improvement acquisition function can be expressed as follows,

$$\begin{aligned} cEI(x) &= E[\tilde{I}_{\mathbf{c}}(x)|x] = E[1_{\mathbf{c}(x)<0}\tilde{I}(x)|x] \\ &= E[1_{\mathbf{c}(x)<\mathbf{0}}|x] \times E[\tilde{I}(x)|x] \\ &= \prod_{r=1}^{R} pr(c_r(x) \leq 0) \times EI(x), \end{aligned}$$

where $pr(c_r(x) \leq 0)$ is a Gaussian probability and represents the probability of feasibility of each constraint function r at point x. The CDF (i.e., cumulative distribution function) of each constraint function is then used as the probability of feasibility of each acquired point as shown in Equations 11 and 12.

$$pr(c_r(x) \leq 0) = \Phi\left(\frac{\mu_r(x)}{\sigma_r(x)}\right), \tag{11}$$

$$cEI(\boldsymbol{x}) = EI(\boldsymbol{x}) \times \prod_{r=1}^{R} \Phi\left(\frac{\mu_r(x)}{\sigma_r(x)}\right), \tag{12}$$

where $\Phi\left(\frac{\mu_r(x)}{\sigma_r(x)}\right)$ represents the CDF of constraint function r, and $\mu_r(x)$ and $\sigma_r(x)$ are the posterior predictive mean and standard deviation of the r^{th} constraint, respectively.

D. Optimization Algorithm

We utilize the proposed constrained Bayesian optimization to minimize the objective function while satisfying a set of physical constraints. As we mentioned earlier, In this setting, both the objective and set of constraint functions are modeled as Gaussian processes. The optimization process starts with obtaining initial design points that are sampled randomly from the input design search space. The GP priors are then updated and used, with the help of the constrained expected improvement acquisition function, to infer the next design point to be evaluated. The optimization process will then continue until no further evaluations are allowed. Finally, posterior GP models along with the estimated global optimum of the objective function are reported. The use of Gaussian processes as surrogate models highly benefits the optimization process in quantifying uncertainty and in reliable estimation of highly complex response surface functions. A detailed step-by-step documentation of the proposed stress-aware optimal actuator placement framework is shown in Algorithm 1.

Algorithm 1 Stress-Aware Optimal Actuator Placement

Inputs: The displacement matrix U (i.e., Equation 6) and residual stresses S (i.e., Equation 7), the objective function (i.e., δ^2 from Equation 1) and set of constraint functions (i.e., Equations 2 and 3), the input search space (i.e., Equations 4 and 5, a set of (l) initial points $X_l = [\boldsymbol{x}_1, \boldsymbol{x}_2, .., \boldsymbol{x}_l]$ sampled randomly from the input search space, and the maximum number of optimization iterations (B).

1: Find the initial objective function values $f(\boldsymbol{x}_1), f(\boldsymbol{x}_2), .., f(\boldsymbol{x}_l)$.
2: Find the initial constraint functions values $c_r(\boldsymbol{x}_1), c_r(\boldsymbol{x}_2), .., c_r(\boldsymbol{x}_l)$ for every $r \in [1, .., R]$.
3: **for** $b = l + 1, .., B$ **do**
4: Update the hyperparameters set θ for every Gaussian process model.
5: Update the mean and variance of the GP models of the objective and constraint functions.
6: Using cEI (i.e., Equation 12), we select the best point to be evaluated $\boldsymbol{x}_b$ such that $\boldsymbol{x}_b = argmax\ cEI(\boldsymbol{x})$ for $\boldsymbol{x} \in \mathcal{D}_{\mathcal{X}}$.
7: Find the values of $f(\boldsymbol{x}_b)$ and $c_r(\boldsymbol{x}_b)$ at $\boldsymbol{x}_b$ for each constraint r.
8: Evaluate $y_b = f(\boldsymbol{x}_b) + \varepsilon_b$
9: Update the mean and variance of the GP model of the response y.
10: Find the so far optimal y^* at input design point $\boldsymbol{x}^*$.
11: **end for**
12: **Return** The global optimum y^* (i.e., the minimum mean squared deviations) at input design point $\boldsymbol{x}^*$ (i.e., optimal actuator forces and locations), and the values of the constraint functions at $\boldsymbol{x}^*$ (i.e., the optimal number of placed actuators and the resulting residual stresses).

III. Case Study: The Placement of Actuators on Composite Fuselages

In this section, we formulate the placement of actuators problem in the aerospace manufacturing in Subsection III-A, discuss the process of parameter estimation and optimization model specifications in Subsection III-B, and finally, we show the results in Subsection III-C.

A. Problem Formulation

The placement of actuators on composite fuselages is an extremely challenging problem. Physical constraints on the location of actuators play an important role in assuring the quality and life-cycle reliability of a composite fuselage. Restrictions to the possible locations of actuators, applied forces, and resulting residual stresses are physical constraints that restrain the placement of actuators process. Taking these factors into consideration, we design our problem as follows: (1) we have 18 limited possible locations of actuators (i.e., due to the engineering constraints, these 18 locations are dispersed on the lower bottom edge of the fuselage), (2) we seek to place a maximum of 10 actuators from these 18 possible locations, (3) we specify lower (i.e., -200 lbs) and upper (i.e., 200 lbs) limits on each actuator force, and (4)

we use the max Tsai-Wu [9] values for estimating residual stresses and to be more conservative, we specify the safety threshold to be 0.3.

B. Parameter Estimation and Optimization Model Specifications

We estimate the displacement matrix U and residual stresses S using Equations 6 and 7. We train the Gaussian process regression model with Matern 5/2 using 40 training fuselages. Next, we evaluate the trained models using 20 testing fuselages and achieve a mean squared error (MSE) of 0.0088 and a mean absolute error (MAE) of 0.0532 for the multivariate linear regression model, shown in Equation 6, and an MSE of 0.00005 and an MAE of 0.0052 for the Gaussian process regression model, shown in Equation 7. From these results, we can find that the prediction accuracy of the Gaussian process model is higher than that of the multivariate linear regression model.

In our constrained Bayesian optimization algorithm, we use Gaussian processes as surrogate models. Specifically, we use Matern 5/2 as the kernel function along with the standard constant (i.e., zero) mean function. We use 1000 maximum optimization iterations with one initial point sampled randomly from the input search space.

C. Results and Discussion

We evaluate our proposed stress-aware optimal actuator placement framework using the 20 testing fuselages. We compare the stress-aware optimal placement with the best fixed actuator placement [15] and the sparse learning based approach [17]. For comparison purposes, we use eight metrics namely, mean and maximum root mean squared deviations (RMSD), mean and maximum of maximum applied absolute forces (MF), mean and maximum number of actuators (NA), and mean and maximum of maximum stresses (MS).

The results of the placement of actuators process for the three benchmarks are shown in Table I. From Table I, we conclude that our proposed stress-Aware optimal actuator placement framework outperforms the other two benchmarks. More precisely, we show significant reductions of at least 39.3% in mean RMSD and 8.7% in maximum RMSD (inches) and at least 23.1% reduction in mean MF (lbf) and 52% reduction in maximum MF (lbf). Only 8 actuators are needed on average and a maximum 9 actuators are needed for the optimal placement process. The mean and maximum of maximum residual stresses are 0.04 and 0.0809 inverse reserve factor (IRF), respectively.

We also compare the stress-aware optimal actuator placement strategy with the MGP-CBO approach without considering internal stresses [19]. The results can be found in Table II. The MGP-CBO is a non-stationary constrained Bayesian optimization model used to infer and represent expensive-to-evaluate non-stationary response surface functions. Although residual stresses incorporation has made the problem of actuators placement extremely complex and challenging, the proposed stress-aware optimal actuator placement outperformed MGP-CBO in terms of the mean RMSD. While other comparison metrics seem comparable, the inclusion of residual stresses will definitely improve the quality of the composite structure which in turn results in a better reliable part.

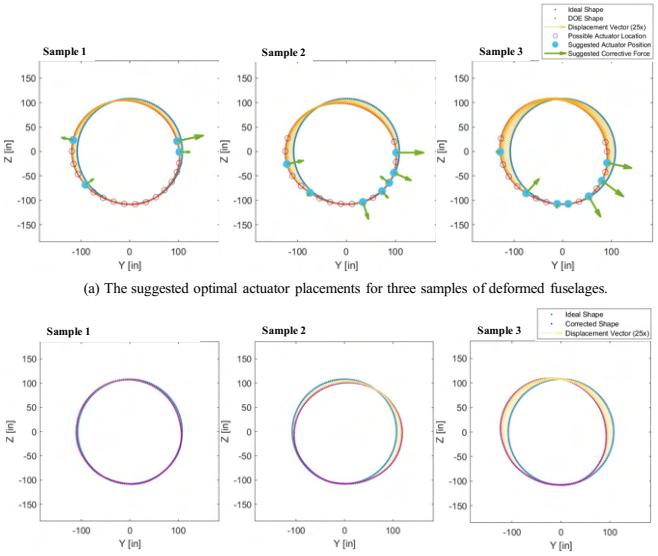

(a) The suggested optimal actuator placements for three samples of deformed fuselages.

(b) The final corrected shape of three samples of fuselages after suggested forces are applied.

Fig. 4. **Validation of the proposed stress-aware optimal actuator placement framework.**

IV. Inference and Validation

In this section, we validate our proposed stress-aware optimal actuator placement framework. Specifically, we perform another finite element simulation to verify the results we obtained in Table I by applying the suggested optimal actuator forces and their locations to the deformed fuselages we used in the optimization procedure. The simulation setup is reflected in Fig. 4 (a), which illustrates our proposed actuator locations and forces for correcting the shape deviations from the DOE for three test samples. In Fig. 4 (b), we show the final fuselage shapes after applying the suggested actuator forces to the DOE shapes. In these examples, the final shape RMSD errors are respectively reduced by 76.9%, 26.2%, and 18.0% compared to the starting (DOE) configuration. We also show, based on these suggested optimal actuator forces and locations, the resulting stress maps in Fig. 5. We find that the Tsai-Wu IRF values observed are at most on the order of 0.1, which leaves a conservative safety margin for the shape adjustment during the assembly step. We note that peak values of stress often arise around the supporting fixtures rather than individual actuator locations. This may be attributed to the avoidance of large forces at individual actuator locations during the optimization procedure. [Note: interactive figures of the validation results can be found in the Multimedia appendix.]

V. Conclusion

In the process of actuators placement on composite structures, high residual stresses due to large forces and de-

TABLE I

COMPARISON RESULTS OF THREE ACTUATOR PLACEMENT METHODS.

Benchmark	Mean RMSD	Max RMSD	Mean MF	Max MF	Mean NA	Max NA	Mean MS	Max MS
Best Fixed Placement	0.0034	0.0062	291.0714	449.6754	10	10	-	-
Sparse Learning Placement	0.0028	0.0046	231.2973	397.9796	10	10	-	-
Stress-Aware Optimal Placement	0.0017	0.0042	177.9724	191.0035	8	9	0.0400	0.0809

TABLE II

COMPARISON RESULTS OF THE MGP-CBO AND STRESS-AWARE OPTIMAL PLACEMENT.

Benchmark	Mean RMSD	Max RMSD	Mean MF	Max MF	Mean NA	Max NA	Mean MS	Max MS
MGP-CBO	0.0020	0.0042	178.8052	190.5369	8	9	-	-
Stress-Aware Optimal Placement	0.0017	0.0042	177.9724	191.0035	8	9	0.0400	0.0809

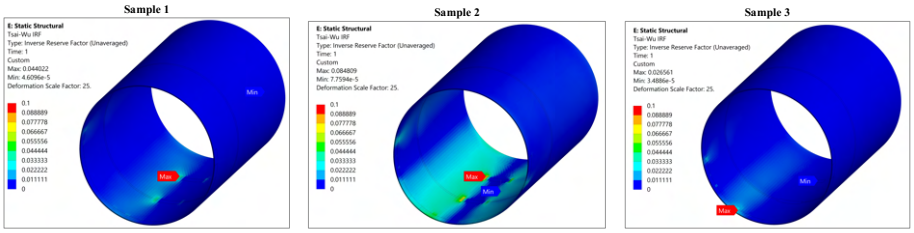

Fig. 5. **The resulted residual stresses on three samples of fuselages after suggested actuator forces are applied.**

formations can cause damage to the inner matrix of the composite structure resulting in micro-cracking and possible catastrophic failure of the part. Hence, incorporation of these residual stresses when optimizing the location of actuators is paramount to the ultra-high precision quality control of composite structures. In this paper, we proposed a *Stress-Aware Optimal Actuator Placement* framework. Utilizing Bayesian optimization models and Gaussian processes, the proposed optimization framework was able to add flexibility to the number of placed actuators while satisfying the residual stresses safety threshold. We compared our proposed optimization framework with two state-of-the-art optimal placement policies in advanced aircraft assembly and showed significant improvements. Specifically, the proposed framework was able to achieve significant reductions of at least 39.3% in mean RMSD (inches) and 52% in maximum MF (lbf). Moreover, while satisfying residual stresses safety threshold, the proposed optimization framework was able to achieve these significant improvements at only 8 actuators on average. The validation simulations were carried out to verify the results obtained by the proposed framework.

REFERENCES

[1] T. W. Clyne and D. Hull, *An introduction to composite materials*. Cambridge university press, 2019.

[2] S. W. Tsai and H. T. Hahn, *Introduction to composite materials*. Routledge, 2018.

[3] J. Sloan, "Composites end markets: Aerospace (2022)," https://www.compositesworld.com/articles/the-markets-aerospace-2022, accessed: 2022-02-25.

[4] Boeing, "Boeing 787: From the ground up," https://www.boeing.com/commercial/aeromagazine /articles/qtr_4_06/article_04_2.html, accessed: 2022-02-25.

[5] J. Sloan, "Boeing conducts inspections of 787 composite inner fuselage skin," https://www.compositesworld.com/news/boeing-conducts-inspections-of-787-composite-inner-fuselage-skin, accessed: 2022-02-25.

[6] D. Gates, "Boeing finds 787 pieces aren't quite a perfect fit," https://www.seattletimes.com/business/boeing-finds-787-pieces-arent-quite-a-perfect-fit/, accessed: 2022-02-25.

[7] R. Hill, *The mathematical theory of plasticity*. Oxford university press, 1998, vol. 11.

[8] Z. Hashin and A. Rotem, "A fatigue failure criterion for fiber reinforced materials," *Journal of Composite Materials*, vol. 7, no. 4, pp. 448–464, 1973.

[9] S. W. Tsai and E. M. Wu, "A general theory of strength for anisotropic materials," *Journal of Composite Materials*, vol. 5, no. 1, pp. 58–80, 1971.

[10] A. Ali, E. Ghotbi, and A. K. Dhingra, "Optimum placement of actuators in structural and control design using stackelberg games," *Journal of Vibration and Control*, vol. 21, no. 7, pp. 1373–1382, 2015.

[11] P. V. Chanekar, N. Chopra, and S. Azarm, "Optimal actuator placement for linear systems with limited number of actuators," in *2017 American Control Conference (ACC)*, 2017, pp. 334–339.

[12] J. Chen, J. Jiang, K. Wang, and F. Zhang, "Optimal placement of actuators for active vibration control using eer and genetic algorithm," in *2019 IEEE 10th International Conference on Mechanical and Aerospace Engineering (ICMAE)*, 2019, pp. 449–453.

[13] A. K. DHINGRA and B. H. LEE, "Optimal placement of actuators in actively controlled structures," *Engineering Optimization*, vol. 23, no. 2, pp. 99–118, 1994.

[14] Y. Wen, X. Yue, J. Hunt, and J. Shi, "Feasibility analysis of composite fuselage shape control via finite element analysis," *Journal of Manufacturing Systems*, vol. 46, pp. 272–281, 2018.

[15] X. Yue, Y. Wen, J. Hunt, and J. Shi, "Surrogate model-based control considering uncertainties for composite fuselage assembly," *Journal of Manufacturing Science and Engineering-Transactions of The ASME*, vol. 140, p. 041017, 2018.

[16] X. Yue and J. Shi, "Surrogate model–based optimal feed-forward control for dimensional-variation reduction in composite parts' assembly processes," *Journal of Quality Technology*, vol. 50, no. 3, pp. 279–289, 2018.

[17] J. Du, X. Yue, J. Hunt, and J. Shi, "Optimal placement of actuators via sparse learning for composite fuselage shape control," *Journal of Manufacturing Science and Engineering-Transactions of The ASME*, vol. 141, 2019.

[18] J. R. Gardner, M. J. Kusner, Z. Xu, K. Q. Weinberger, and J. Cunningham, "Bayesian optimization with inequality constraints," in *International Conference on Machine Learning (ICML)*, 2014.

[19] A. AlBahar, I. Kim, X. Wang, and X. Yue, "Physics-constrained bayesian optimization," *Technical Report*, 2021.